The Plant Cell, Vol. 27: 2469–2483, September 2015, www.plantcell.org

The Interaction between Rice ERF3 and WOX11 Promotes Crown Root Development by Regulating Gene Expression Involved in Cytokinin Signaling[OPEN]

Yu Zhao,[a,1,2] Saifeng Cheng,[a,2] Yaling Song,[a] Yulan Huang,[a] Shaoli Zhou,[a] Xiaoyun Liu,[a] and Dao-Xiu Zhou[a,b]

[a] National Key Laboratory of Crop Genetic Improvement, Huazhong Agricultural University, 430070 Wuhan, China
[b] Institute of Plant Sciences Paris-Saclay (IPS2), Université Paris-Sud 11, 91405 Orsay, France

ORCID IDs: 0000-0003-4451-9907 (Y.Z.); 0000-0003-2712-3521 (S.C.); 0000-0001-9111-1598 (S.Z.); 0000-0002-5740-9777 (X.L.); 0000-0002-1540-0598 (D.-X.Z.)

Crown roots are the main components of the fibrous root system in rice (*Oryza sativa*). *WOX11*, a *WUSCHEL*-related homeobox gene specifically expressed in the emerging crown root meristem, is a key regulator in crown root development. However, the nature of *WOX11* function in crown root development has remained elusive. Here, we identified a rice AP2/ERF protein, ERF3, which interacts with WOX11 and was expressed in crown root initials and during crown root growth. Functional analysis revealed that *ERF3* was essential for crown root development and acts in auxin- and cytokinin-responsive gene expression. Downregulation of *ERF3* in *wox11* mutants produced a more severe root phenotype. Also, increased expression of *ERF3* could partially complement *wox11*, indicating that the two genes functioned cooperatively to regulate crown root development. *ERF3* and *WOX11* shared a common target, the cytokinin-responsive gene *RR2.* The expression of *ERF3* and *WOX11* only partially overlapped, underlining a spatio-temporal control of *RR2* expression and crown root development. Furthermore, ERF3-regulated *RR2* expression was involved in crown root initiation, while the ERF3/WOX11 interaction likely repressed *RR2* during crown root elongation. These results define a mechanism regulating gene expression involved in cytokinin signaling during different stages of crown root development in rice.

INTRODUCTION

Cereals, such as rice (*Oryza sativa*) and maize (*Zea mays*), have a complex root system structure with several root types, including embryonic primary roots, lateral roots, and shoot-borne roots (also known as adventitious roots). The embryonic primary root develops shortly after germination. Shoot-borne roots initiate from stem nodes or coleoptile sections and are also called crown roots (Marcon et al., 2013). The fundamental difference between cereals and the dicot model plant *Arabidopsis thaliana* is that cereals have an extensive postembryonic crown-borne root system, which Arabidopsis lacks. To date, organization and cell differentiation processes in root development have been well characterized in Arabidopsis (reviewed in Scheres, 2002). During rice root morphogenesis, several developmental stages can be clearly distinguished, including crown root initiation, emergence, and elongation (Itoh et al., 2005; Coudert et al., 2010; Kitomi et al., 2011b; Wang et al., 2011). Although several key genes have been identified and characterized in the regulation of crown root development (Inukai et al., 2005; Liu et al., 2005; Kitomi et al., 2008; Liu et al., 2009; Zhao et al., 2009), the molecular mechanisms of crown root formation and the functional relationship between these genes are not known.

Available evidence indicates that regulation of crown root formation in rice and lateral root formation in Arabidopsis share several common characteristics. For instance, auxin biosynthesis or signaling-related mutants show morphological abnormalities in both rice crown roots and Arabidopsis lateral roots (De Smet and Jürgens, 2007; Kitomi et al., 2011b; Marcon et al., 2013). Exogenous treatment with auxin induces ectopic formation of lateral and adventitious roots in Arabidopsis (Schiefelbein, 2003; Verstraeten et al., 2013). Arabidopsis lateral root regulatory genes *LATERAL ORGAN BOUNDARIES-DOMAIN16/ASYMMETRIC LEAVES2-LIKE18* (*LBD16/ASL18*) and *LBD29/ASL16* are reported to function downstream of *AUXIN RESPONSE FACTOR7* (*ARF7*)- and *ARF19*-dependent auxin signaling (Okushima et al., 2007; Lee et al., 2009; Goh et al., 2012). In rice, mutants or knockdown transgenic plants of genes involved in auxin signaling pathways and/or polar auxin transport (e.g., *CROWN ROOTLESS1* [*CRL1*]/*ADVENTITIOUS ROOTLESS1* [*ARL1*], *CRL4*/*GNOM1*, *CAND1*, *PIN1*, *CRL5*, *Aux*/*IAA3*, and *MANNOSYL-OLIGOSACCHARIDE GLUCOSIDASE*) display reduced or no crown root phenotypes (Inukai et al., 2005; Liu et al., 2005; Xu et al., 2005; Nakamura et al., 2006; Liu et al., 2009; Kitomi et al., 2011a; Wang et al., 2011; Zhu et al., 2012; Wang et al., 2014). In addition, a gain-of-function mutation of *IAA11* affects lateral root development in rice (Nakamura et al., 2006; Zhu et al., 2012).

Cytokinin, which acts antagonistically to auxin, plays an important role in controlling root growth during postembryonic development. Cytokinin stimulates cell differentiation in the root proximal meristem, which leads to a decrease of meristem size

[1] Address correspondence to zhaoyu@mail.hzau.edu.cn.
[2] These authors are co-first authors.
The author responsible for distribution of materials integral to the findings presented in this article in accordance with the policy described in the Instructions for Authors (www.plantcell.org) is: Yu Zhao (zhaoyu@mail.hzau.edu.cn).
[OPEN]Articles can be viewed online without a subscription.
www.plantcell.org/cgi/doi/10.1105/tpc.15.00227

and root growth (Dello Ioio et al., 2007, 2008; Bishopp et al., 2009; Ruzicka et al., 2009; Moubayidin et al., 2010). Mutations of Arabidopsis type-A cytokinin response factor genes *ARR7* and *ARR15* lead to misexpression of root development regulatory genes, such as *SCARECROW*, *PLETHORA1* (*PLT1*), and *WUSCHEL-RELATED HOMEOBOX5* (*WOX5*) (Lee et al., 2013; Müller and Sheen, 2008). Knockdown or overexpression of rice genes involved in cytokinin signaling pathway also affects root development. For instance, *RR3* and *RR5* overexpression plants produce more and longer lateral roots compared with the wild type when treated with exogenous cytokinin (Cheng et al., 2010). Overexpression of *RR6* leads to dwarf phenotype with a poorly developed root system (Hirose et al., 2007).

Auxin-cytokinin crosstalk plays an important role in the regulation of root meristem activities (Müller and Sheen, 2008; Benková and Hejátko, 2009; Su et al., 2011; Durbak et al., 2012). Recent progress has revealed that the balance between cell differentiation and division, which is necessary for controlling root meristem size and root growth, is regulated by antagonistic action of cytokinin and auxin in Arabidopsis and rice (Dello Ioio et al., 2007; Kitomi et al., 2011b; Gao et al., 2014). In the root meristem, a primary cytokinin-response transcription factor, ARR1, activates *SHORT HYPOCOTYL2/IAA3*, a repressor of auxin signaling that negatively regulates the *PIN* auxin transport facilitator genes (Dello Ioio et al., 2008). Recent work reported that *CYTOKININ OXIDASE4* mediates crown root development by integrating the interaction between cytokinin and auxin (Gao et al., 2014). We previously showed that rice *WOX11*, which belongs to the WOX transcription factor family, is involved in the activation of crown root development by regulating genes of both auxin and cytokinin signaling (Zhao et al., 2009). In this work, we identified the rice AP2/ETHYLENE-RESPONSIVE FACTOR (ERF) protein, ERF3, as a WOX11-interacting partner involved in rice crown root development. Our results showed that *ERF3* was involved in crown root initiation and elongation. Further analysis indicated that ERF3 stimulated the expression of type-A *RR* gene *RR2* in crown root initials. Overexpression of *RR2* also promoted crown root initiation. Our data suggested that ERF3 regulation of crown root initiation may involve cytokinin signaling and that its interaction with WOX11 might enhance WOX11-mediated repression of *RR2* or inhibit its function on *RR2* activation during crown root elongation.

RESULTS

Identification of ERF3 as a WOX11-Interacting Protein

To elucidate the molecular basis by which *WOX11* controls crown root development, yeast two-hybrid screening of WOX11-interacting proteins were performed using a rice root tip cDNA library. With the full-length *WOX11* cDNA as bait, a total of 36 positive clones were isolated from the screening, which corresponded to 19 genes. One of the genes encoded ERF3 (*Os01g58420*), which accounted for nearly one-seventh (5 of 36) of all the positive clones. The clones isolated from the screening contained the whole coding region of *ERF3*. To validate the

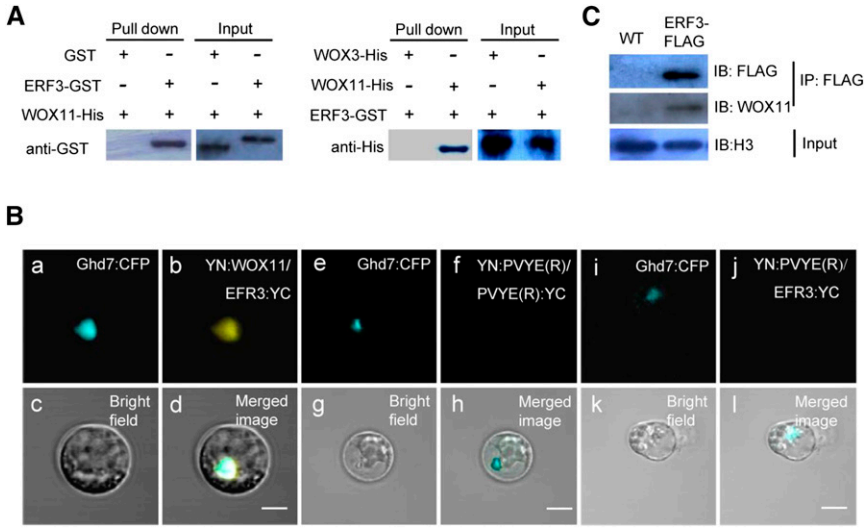

Figure 1. ERF3 Directly Interacts with WOX11 in Vitro and in Vivo

(A) Pull-down assay of ERF3 interaction with WOX11. Left, ERF3-GST fusion protein or GST alone were incubated with WOX11-His in His beads. ERF3-GST but not GST was pulled down by the beads containing WOX11-His. Right, WOX11-His and WOX3-His were incubated with EFR3-GST in GST beads. WOX11-His but not WOX3-His was pulled down by the beads containing ERF3-GST.

(B) Interaction of ERF3 and WOX11 in rice protoplasts. Representative cells are shown, as imaged by confocal laser scanning microscopy. a, e, and i, Ghd7: CFP localization in the nucleus (blue fluorescence); b, detection in rice protoplasts of YN:WOX11 and ERF3:YC interaction, shown as yellow signal; f and j, as negative controls with YN:pVYNE(R)/pVYCE(R):YC and YN: pVYNE(R)/ERF3:YC; c, g, and k, bright field; d, h, and l, colocalization of three signals is indicated in merged images. Bars = 10 μm.

(C) In vivo coimmunoprecipitation assay of ERF3 and WOX11 interaction. Roots of 10-d-old seedling of ERF3-FLAG transgenic plants and the wild type (WT) were immunoprecipitated (IP) using an anti-FLAG polyclonal antibody and immunoblotted (IB) using anti-FLAG or anti-WOX11 antibodies as indicated.

yeast two-hybrid data, both in vitro and in vivo experiments were performed to test the ERF3-WOX11 interaction. Recombinant full-length ERF3 and glutathione *S*-transferase (GST) fusion protein and the full-length WOX11 tagged with 6×His were produced in *Escherichia coli* and purified. His pull-down assays showed that ERF3-GST but not GST was retained by WOX11 (Figure 1A, left). Conversely, pull-down assays with GST revealed that WOX11-6×His but not WOX3-6×His was retained by ERF3 protein (Figure 1A, right) (Dai et al., 2007). To further confirm the interaction, bimolecular fluorescence complementation (BiFC) assays were performed in rice protoplasts. YFP was reconstituted when the coding sequences of *ERF3* and *WOX11* were coexpressed (Figure 1B, a to d). In contrast, coexpression of the ERF3-YFP C terminus and YFP-N terminus (Figure 1B, e to h), or the YFP protein C terminus and N terminus alone, did not show fluorescence (Figure 1B, i to l), which confirmed that the ERF3-WOX11 interaction is specific. Moreover, the BiFC experiments clearly revealed that ERF3-WOX11 interacted in the nucleus (Figure 1B, a to d), as YFP fluorescence fully overlapped with the nuclear protein Ghd7 (Xue et al., 2008) fused to CFP.

Coimmunoprecipitation assays were performed to confirm the interaction between ERF3 and WOX11 in rice cells. Stable transgenic rice plants expressing ERF3-FLAG (under the maize *ubiquitin* promoter) were generated (Supplemental Figure 1). Crude protein extracts of roots from ERF3-FLAG and wild-type plants were immunoprecipitated by anti-FLAG antibody and then analyzed by immunoblotting with anti-FLAG and anti-WOX11 antibodies. As shown in Figure 1C, both ERF3-FLAG and WOX11 proteins were detected, further confirming the in vivo interaction between the two proteins.

ERF3 Displays a Partially Overlapping Expression Pattern with *WOX11* in Developing Crown Roots and Is Responsive to Auxin and Cytokinin

To study *EFR3* expression, we first examined *ERF3* mRNA accumulation in various organs/tissues at different developmental stages by RT-qPCR. The analysis showed that *ERF3* was broadly expressed (Figure 2A). To gain insight into the functional significance of the interaction between ERF3 and WOX11, we further explored the expression pattern of *ERF3* during rice crown root

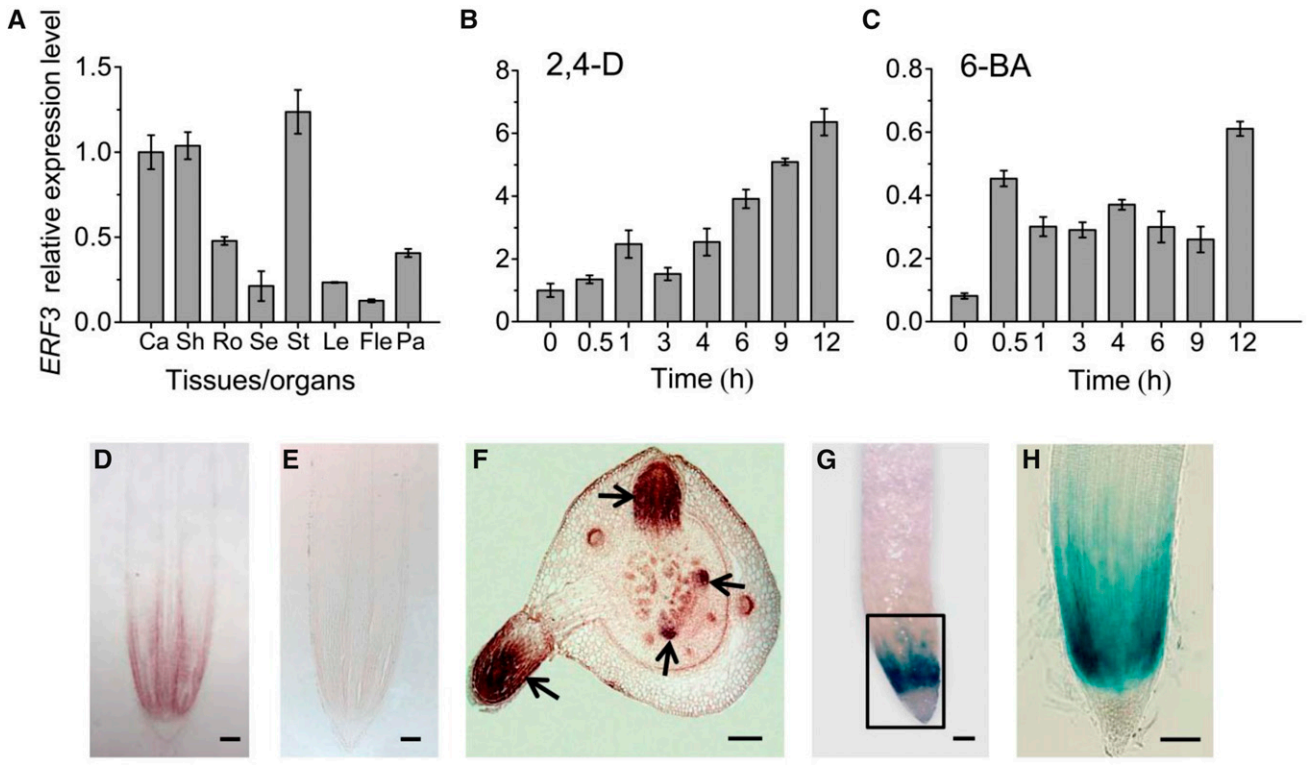

Figure 2. *ERF3* Expression in Rice Crown Root Development.

(A) Detection of *ERF3* expression by RT-qPCR in callus (Ca), shoot (Sh), root (Ro), seedling (Se), stem (St), leaf (Le), flag leaf (Fle), and panicle (Pa). *ACTIN1* was used as an internal control. Bars are means ± SD from three technical replicates.

(B) and **(C)** Kinetics of induction of *ERF3* in response to plant hormones 2,4-D and 6-BA. The transcript level of *ERF3* in roots of 10-d-old light-grown wild-type seedlings treated with 2,4-D or 6-BA for the indicated times were plotted as the relative expression (fold) of water-treated seedling during the same durations. The PCR signals were normalized with those of the *ACTIN1* transcripts. Bars are means ± SD from three technical replicates.

(D) to **(F)** In situ hybridization detection of *ERF3* transcripts in crown root tip **(D)** and primordia **(F)** with an antisense or a sense probe **(E)**. Arrows indicate crown root initials at different stages. Bars = 25 μm.

(G) and **(H)** GUS activity in crown root tip. **(H)** is the boxed region in **(G)**. Bars = 75 μm

development by in situ hybridization and promoter-reporter lines. The results indicated that *ERF3* was preferentially expressed in crown root initials, the crown root meristem (cell division) region, and in elongating crown roots (Figures 2D and 2F). This expression pattern overlapped with that of *WOX11* but displayed some differences during crown root development, as *WOX11* is expressed mainly after crown roots emergence and is hardly detectable in crown root initials (Zhao et al., 2009). In the promoter-reporter

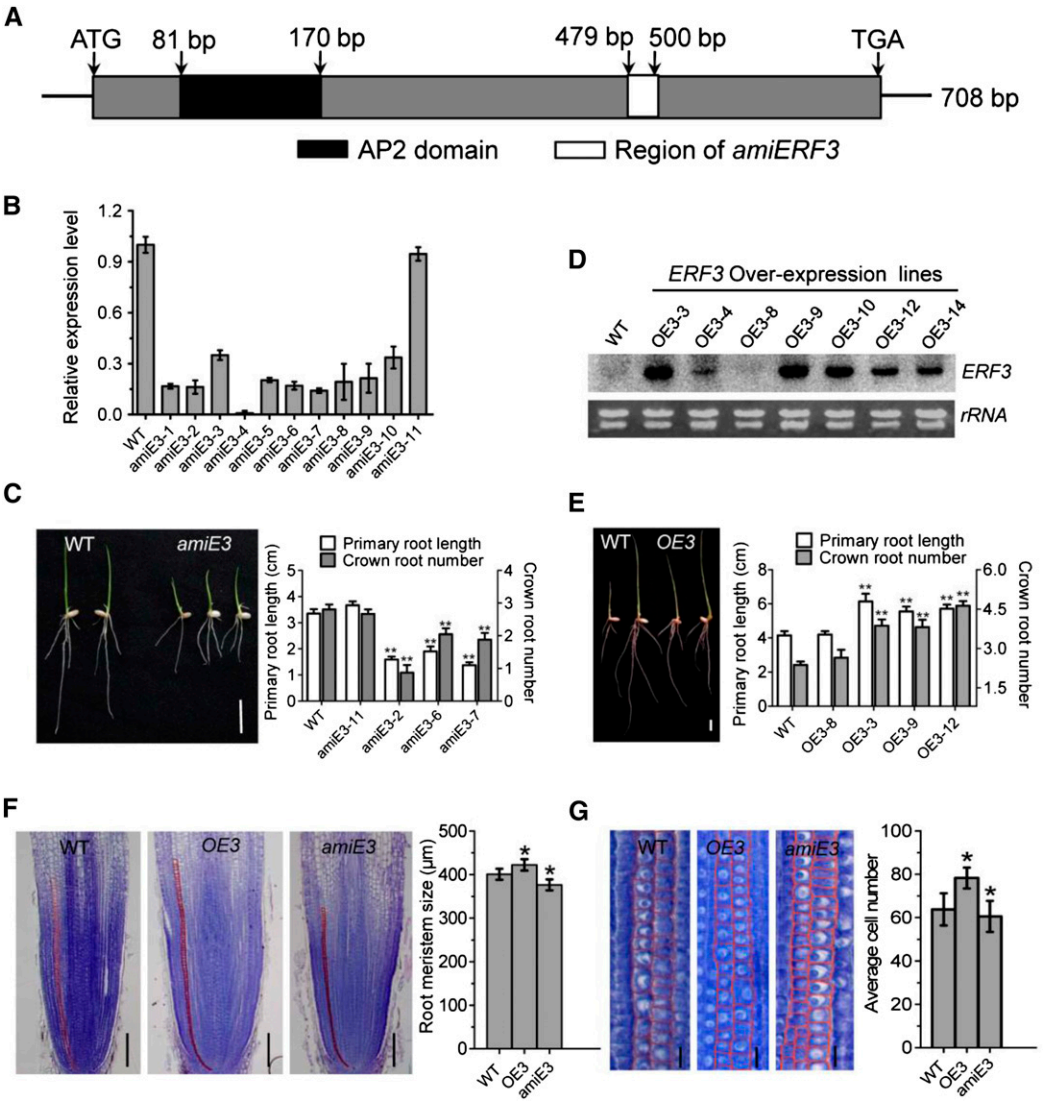

Figure 3. Analysis of *ERF3* amiRNAs and Overexpression Transgenic Plants.

(A) Schematic representation of the *ERF3* cDNA. The black box corresponds to the conserved domain (AP2 domain). The cDNA region used to construct the artificial microRNAs vector is indicated by the white box.

(B) RT-qPCR analysis of *ERF3* transcripts in the wild type and 11 amiRNA (*amiE3*) transgenic lines. The PCR signals were normalized with *ACTIN1* transcripts. Transcript level from the wild type was set at 1. Bars are means ± SD from three technical replicates.

(C) Comparison of primary root length and crown root number of 1-week-old seedlings between the wild type (WT; left) and the amiRNA line (*amiE3*; right). Picture and statistical data were taken from lines *amiE3*-2, *amiE3*-6, and *amiE3*-7, which showed similar phenotypes. *amiE3*-11 was used as a negative control. Bar = 1 cm.

(D) RNA gel blot analysis of *ERF3* overexpression plants (*OE3*) in different transgenic lines compared with the wild type. The rRNA levels were revealed as controls. Statistical analyses of the data in **(C)** and **(D)** are presented in Table 1.

(E) Comparison of primary root length and crown root number of 1-week-old seedlings between wild-type (left) and overexpression plants (*OE3*; right). Picture and statistical data were taken from lines *OE3*-3, *OE3*-9, and *OE3*-12, which showed similar phenotypes. *OE3*-8 was used as a negative control. Bar = 1 cm.

(F) and **(G)** Histological analysis of crown root tip in the wild type, *ERF3* amiRNAs (*amiE3*), and overexpression plants (*OE3*). Red lines delimit the meristem size (i.e., the distance between the quiescent center and the transition zone) **(G)**. Cell number in meristem zone of wild-type, *ERF3* overexpression (*OE3*), and amiRNA (*amiE3*) roots. Statistical analyses (*t* test) of data in **(F)** and **(G)** were performed with the wild type ($n = 16$), *ERF3* overexpression (*OE3*; $n = 20$), and amiRNAs (*amiE3*; $n = 17$). Error bars in **(F)** and **(G)** represent SD. *$P < 0.05$.

Table 1. Comparison of Primary Root Length and Crown Root Number between the Wild Type, *ERF3* Overexpressing (*OE3*), and RNAi Transgenic Lines (*amiE3*) 2 Weeks after Germination

Genotype (Plant Number)	Primary Root Length (cm)	Crown-Borne Root Number
Wild type (20)	9.43 ± 0.38	4.96 ± 0.24
amiE3-11 (16)	9.02 ± 0.28	5.02 ± 0.23
amiE3-2 (24)	5.04 ± 0.25**	2.71 ± 0.46**
amiE3-6 (17)	5.78 ± 0.49**	4.06 ± 0.39*
amiE3-7(21)	5.65 ± 0.36**	4.00 ± 0.27*
OE3-8 (14)	9.61 ± 0.37	5.02 ± 0.15
OE3-3 (17)	13.97 ± 0.35**	6.21 ± 0.11*
OE3-9 (13)	14.55 ± 0.33**	5.97 ± 0.29*
OE3-12 (29)	13.82 ± 0.33**	6.25 ± 0.21*

Significant differences are indicated at the 5% (*) and 1% (**) probability levels (two-tailed *t* test). *amiE3*-11 and *OE3*-8 are negative controls.

lines, GUS activity was mainly detected in the cell division zones of the primary root meristem (Figures 2G and 2H). This expression profile suggested that *ERF3* and *WOX11* might be involved in different stages of crown root development. The colocalization of *WOX11* and *ERF3* suggested that the ERF3-WOX11 pairs may function in rice crown root formation.

As *WOX11* expression is regulated by auxin and cytokinin, we wanted to know whether *ERF3* was also regulated by these two hormones. Wild-type seedlings (10 d after germination) were transferred to liquid media containing 10^{-6} M 2,4-D or 10^{-5} M 6-benzylaminopurine (6-BA). The roots were harvested for RNA extraction at 0, 0.5, 1, 3, 4, 6, 9, and 12 h after hormone treatment. It is noteworthy that *ERF3* transcript was induced by both 2,4-D and 6-BA after 1 or 0.5 h treatment, respectively (Figures 2B and 2C), suggesting that *ERF3* responds to auxin and cytokinin signaling pathways.

Knockdown and Overexpression of *ERF3* Affect Crown Root Formation in Rice

To study the function of *ERF3* in rice root development, we generated transgenic plants expressing *ERF3* artificial microRNAs (*amiE*3) (Figure 3A). Expression analysis of the transgenic population led to the identification of 10 lines (*amiE3*-1- *amiE3*-10) with reduced *ERF3* mRNA levels (Figure 3B). Three of the artificial microRNA (amiRNA) lines (*amiE3*-2, *amiE3*-6, and *amiE3*-7) were selected for subsequent analysis. Line *amiE3*-11, which did not show any reduction of *ERF3* transcripts, was used as a negative control in subsequent analysis (Figure 3B). Seven days after germination, the *amiERF3* seedlings developed fewer crown roots than the wild type (Figure 3C). In addition, the primary root length and the plant height were also reduced (Figure 3C). Fourteen days after germination, the primary root length of the *amiERF3* plants remained significantly shorter and the crown root number was reduced compared with the wild type (Table 1). To check if *ERF3* regulated the initiation of crown root primordia, cross sections of the coleoptilar nodal region of 3- and 5-d-old seedlings were stained with toluidine blue. Crown roots were not initiated or retarded in *amiERF3* transgenic lines compared with the wild type (Supplemental Figure 2B), indicating that *ERF3* was essential for primary root elongation and crown root initiation.

To further confirm *ERF3* function in root development, a vector containing the *ERF3* cDNA under the control of the maize *ubiquitin* promoter was transformed into rice plants. RNA gel blot analysis revealed that several transgenic lines showed *ERF3* overexpression (Figure 3D). Three overexpression lines (*OE3*-3, *OE3*-9, and *OE3*-12) and one negative transgenic line (*OE3*-8) were selected for further analysis. The overexpression plants produced a larger root system (with more and longer roots) 7 d after germination compared with the wild type and the transgenic negative control line (Figure 3E). Fourteen days after germination, the overexpression plants developed more crown roots and longer primary roots compared with the wild type and the control line (Table 1). These data suggested that elevated *ERF3* expression level promoted crown root initiation and elongation in rice.

To study whether *ERF3* regulated root meristem size, longitudinal sections of root tip of wild-type, *amiERF3* (*amiE3*), and *ERF3* overexpression (*OE3*) transgenic lines were stained with toluidine blue (Figure 3F). The root meristem of *OE3* plants was longer than that of wild-type and *amiERF3* plants (wild type, 400.71 ± 12.55; *OE3*, 422.29 ± 13.07*; *amiE3*, 376.38 ± 12.5*; data were obtained from three lines for each transgenic genotype with $n > 15$ for each line). Because root meristem size is correlated with the cell number in the meristem region and cell longitudinal length, examination of longitudinal section revealed that the root meristem of *OE3* plants contained more cells (*OE3*, 78.77 ± 8.78**; wild type, 63.77 ± 12.4) and the cell longitudinal size was longer than that of the wild type (*OE3*, 11.25 ± 0.78*; wild type, 9.02 ± 0.40). While in *amiERF3* plants root meristem, there were fewer cells (60.5 ± 9.16**) and shorter cell longitudinal length (8.03 ± 0.17*) compared with the wild type (Figure 3G; Supplemental Figure 2). These data suggested that *ERF3* was likely to be involved in promoting both cell division and cell longitudinal elongation of the root meristem in rice.

ERF3 Functions in Regulating Expression of Crown Root Developmental and Hormone-Responsive Genes

The *CRL1*, *CRL4/GNOM1*, *CRL5*, and *WOX11 g*enes are involved in different regulatory pathways of crown root initiation and growth (Inukai et al., 2005; Liu et al., 2005; Kitomi et al., 2008, 2011a; Liu et al., 2009; Zhao et al., 2009). To determine whether *ERF3* regulates these genes, we analyzed their mRNA levels in the roots of *ERF3* transgenic plants. RT-qPCR results showed that *CRL1*, *CRL4/GNOM1*, and *CRL5* were highly induced in *ERF3* overexpression lines. In the *amiERF3* lines, *CRL1* and *CRL4/GNOM1* were repressed but *CRL5* was upregulated, suggesting that *EFR3* might be directly or indirectly involved in regulation of these genes. However, *WOX11* expression was not clearly affected in the transgenic plants (Figure 4A), suggesting that *ERF3* was not involved in the regulation of *WOX11*.

To determine whether *ERF3* was also involved in auxin and cytokinin signaling, we analyzed the expressions of four auxin-responsive *Aux/IAA* genes (*IAA5*, *IAA11*, *IAA23*, and *IAA31*) and four cytokinin-responsive type-A *RR* genes (*RR1-RR4*) in 7-d-old seedling root tips (~8 to 10 mm long) of wild-type, three *amiERF3* (*amiE3*-2, -6, and -7), and three *ERF3* overexpression lines (*OE3*-3, -9, and -12) lines. These genes have been shown to be highly expressed in rice roots and to be regulated by *WOX11* (Jain et al.,

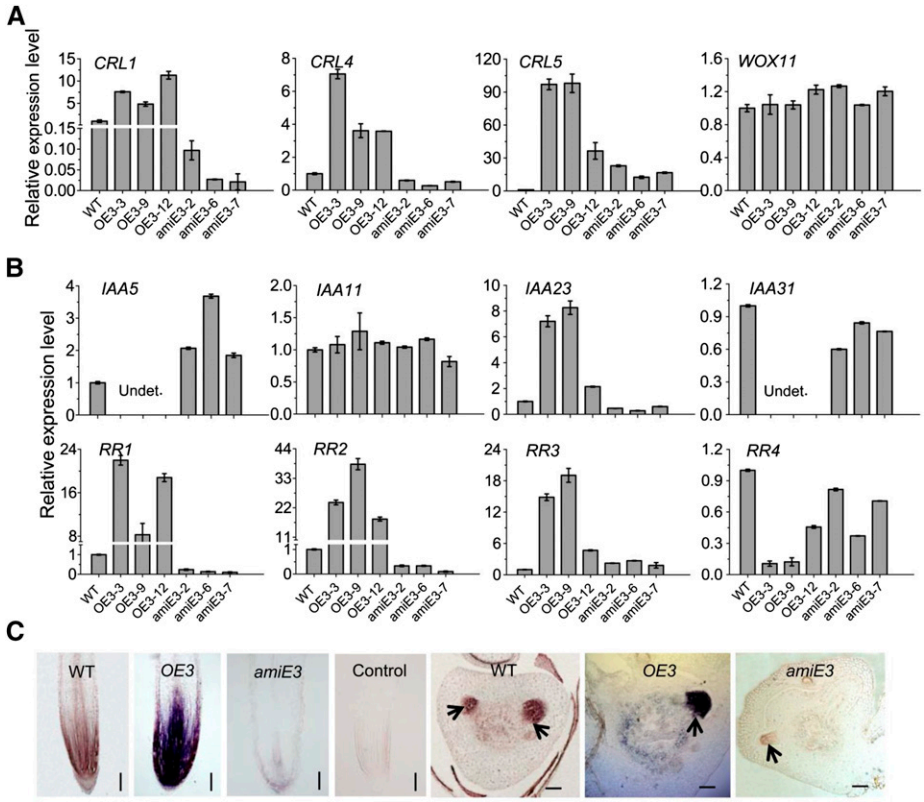

Figure 4. Expression of Root Development and Auxin/Cytokinin Response Genes in Crown Roots of *ERF3* Transgenic Plants.

(A) Relative expression level of root developmental genes determined by RT-qPCR.

(B) Relative expression level of four rice *Aux/IAA* genes and four type-A *RR* genes determined by RT-qPCR.

The PCR signals in **(A)** and **(B)** were normalized with *ACTIN1* transcripts. Transcript level from the wild type was set at 1. *ACTIN1* was used as an internal control. Data represent the means ± SD of three independent biological replicates.

(C) In situ hybridization detection of *RR2* transcripts in the crown root tip and crown root primordia in the wild type (WT), *ERF3* overexpression (*OE3*), and *ERF3* amiRNAs (*amiE3*) with an antisense or sense probe (control). Arrows indicate crown root initials. Bars= 75 μm.

2006; Du et al., 2007; Zhao et al., 2009). We detected the *IAA5* and *IAA31* transcripts in the wild type and *amiEFR3*, but not in the overexpression plants. By contrast, *IAA23* showed higher expression in the *ERF3* overexpression and a lower expression in the *amiEFR3* lines compared with the wild type. *IAA11* displayed no difference in expression level between the transgenic and wild-type plants (Figure 4B). Therefore, up- or downregulation of *ERF3* caused complex changes in the expression pattern of auxin-responsive genes.

Three of the four tested type-A *RR* genes (*RR1*, *RR2*, and *RR3*) were highly upregulated (10- to 40-fold) in the overexpression plants, while *RR1* and *RR2* were repressed in the *amiERF3* lines. However, *RR4* was repressed in both the overexpression and amiRNA lines, with more severe repression observed in the overexpression lines (Figure 4B). Furthermore, in situ hybridization experiments showed that *RR2* had a higher expression in root meristem and crown root initials of *ERF3* overexpression plants and a lower expression in *amiERF3* lines compared with the wild type (Figure 4C). The results suggested that *RR2* might be among immediate targets of *ERF3* and *RR* genes might be subject to complex feedback control of cytokinin and auxin signaling possibly disturbed by up- or downregulation of *ERF3*.

ERF3 Directly Binds to *RR2* and Positively Regulates *RR2* Expression

Our previous studies suggested that WOX11 could bind to the *RR2* promoter region (1092 bp upstream of the ATG) in vitro and in vivo and directly suppresses *RR2* expression in elongating crown roots (Zhao et al., 2009). The expression data shown in Figure 4 suggested that *RR2* might be also targeted by ERF3. ERF proteins bind specifically to the GCC motif (GCCGCC), the core sequence of the ethylene-responsive element (ERE) (Hao et al., 1998). To investigate whether ERF3 directly binds to *RR2*, we analyzed *RR2* genomic sequence and identified three GCC motifs in the *RR2* locus: the first one (P1, 822 bp upstream to ATG) had two GCC repeats (GCCGCC) in the promoter region; the second (P2; 102 bp downstream to ATG) had three GCC repeats (GCCGCCGCC) in the first exon; and the third (P3; 179 bp downstream to ATG) had the two GCC repeats (GCCGCC) located in the first intron of *RR2* (Figure 5A). To examine whether ERF3 protein directly bound to these element sequences, we performed electrophoresis mobility shift assays (EMSAs) using DNA fragments corresponding to P1, P2, and P3 regions and

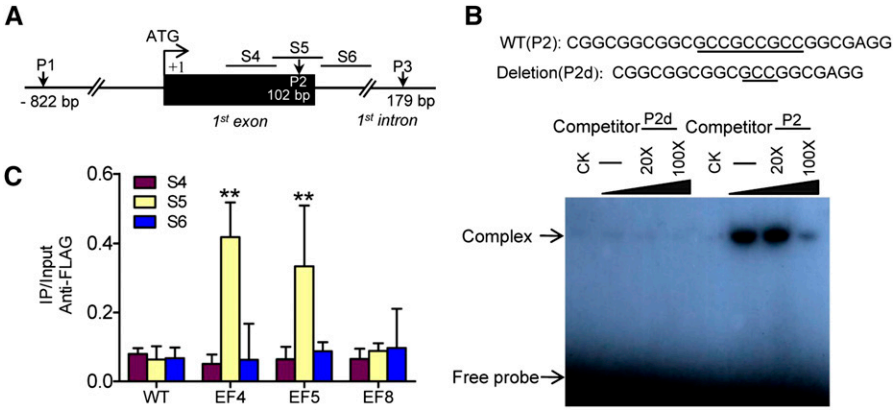

Figure 5. ERF3 Directly Binds to *RR2* in Vitro and in Vivo.

(A) Schematic representation of three putative loci of ERF binding sites in the *RR2* genomic sequence. P1 (−822 bp) including GCCGCC motif, P2 (within the first exon) including GCCGCCGCC motif, and P3 (within the first intron) including GCCGCC motif.

(B) Gel-shift assay of ERF3 protein binding to the first exon sequence (P2) of *RR2* containing the ERF binding site (underlined) or a deletion version (P2d). *E. coli*-produced ERF3 protein was incubated with ^{32}P-labeled P2 or P2d in the absence or presence of 20 or 100 M excess of the corresponding cold probes and analyzed by electrophoresis. The shifted band is indicated by the arrow. Three biological replicates were conducted.

(C) ChIP analysis of transgenic plants expressing ERF3-FLAG fusion protein. Nuclei from three ERF3-FLAG transgenic lines (EF4, EF5 and EF8, EF8 as a negative control) and the wild type (WT) were immunoprecipitated by anti-FLAG or without antibody. The precipitated chromatin fragments were analyzed by qPCR using three primer sets amplifying three *RR2* regions (S4, S5, and S6), as indicated in **(A)**. The relative nucleotide positions of the putative ERF binding site are indicated (with the initiation ATG codon being assessed as +1). One-tenth of the input chromatin was analyzed as control. Error bars represent means ± SD from three independent experiments.

ERF3 protein produced in *E. coli*. As shown in Figure 5B and Supplemental Figure 3, the recombinant ERF3 only bound to P2, but not to P1 or P3. In addition, increasing molar excesses of unlabeled P2 fragment (competitor) inhibited the binding (Figure 5B). Furthermore, deletion of one GCC repeat from P2 also abolished the binding (Figure 5B). These results indicated that ERF3 bound specifically to the P2 site in the first exon of the gene in vitro.

To further confirm whether ERF3 bound to *RR2* in vivo, chromatin fractions from wild-type and two ERF3-FLAG transgenic plants EF4 and EF5 together with a negative control EF8 (Supplemental Figure 1) were isolated and used for chromatin immunoprecipitation (ChIP) with anti-FLAG antibody. The precipitated products in the presence of the antibody as well as input (no antibody) were analyzed by qPCR using three primer sets (S4 to S6) corresponding to different regions around P2 (Figures 5A and 5C). As expected, only the S5 region covering the P2 sequence was clearly precipitated from the two ERF3-FLAG lines. The result indicated that *ERF3* directly bound to *RR2* in vivo.

ERF3 Promotes WOX11 Binding to *RR2* in Vitro and in Vivo

To check whether the ERF3/WOX11 interaction affected their binding to *RR2*, we performed EMSA using DNA fragments containing either the ERF3 (P2) or the WOX11 binding site in the *RR2* genomic region as probes. The assays revealed that the binding of WOX11 to *RR2* was enhanced by ERF3-GST, but not GST tag alone (Figure 6A, left). In contrast, the binding of ERF3-GST to *RR2* was not apparently enhanced by inclusion of WOX11 (Figure 6A, right). These observations suggested that the physical interaction between ERF3 and WOX11 might promote WOX11 binding to the *RR2* gene in vitro.

To confirm the effect of the ERF3/WOX11 interaction on WOX11 binding to *RR2* in vivo, we isolated chromatin fragments from roots of wild-type, *amiERF3*, and *ERF3* overexpression plants and performed immunoprecipitation with the anti-WOX11 antibody. The precipitated products from the three genotypes as well as inputs were analyzed by qPCR using three primer sets (S1 to S3) corresponding to the WOX11 binding region in *RR2*. The results revealed that, compared with the S1 and S3 regions, the S2 region covering the WOX11 binding sequence was enriched in the wild type. The enrichment was greatly enhanced in ERF3 overexpression plants compared with wild-type plants (Figure 6B). These results suggested that ERF3 promoted WOX11 binding to the promoter region of *RR2* in roots. Additionally, chromatin products from wild-type, *wox11*, and *OxWOX11* (*WOX11* overexpression) lines could also be precipitated by anti-ERF3. Further analysis revealed a clear enrichment of ERF3 binding to the S5 region in the first exon of *RR2* compared with S4 and S6 regions in wild-type plants. However, the binding was reduced in *wox11* mutant, but not clearly enriched in *OxWOX11* plants (Figure 6B). The reduction may be due to down-regulation of *ERF3* in *wox11* mutants (Supplemental Figure 4A). These data suggested that ERF3 promoted WOX11 binding to *RR2* in rice roots.

Knockdown of *ERF3* in *wox11* Mutant Background Had a More Severe Effect on Crown Root Growth

The phenotype of *amiERF3*, which showed fewer crown roots and shorter primary roots (Figure 3C), was similar to that of *wox11* mutant (Zhao et al., 2009). Downregulation of *ERF3* had no effect on

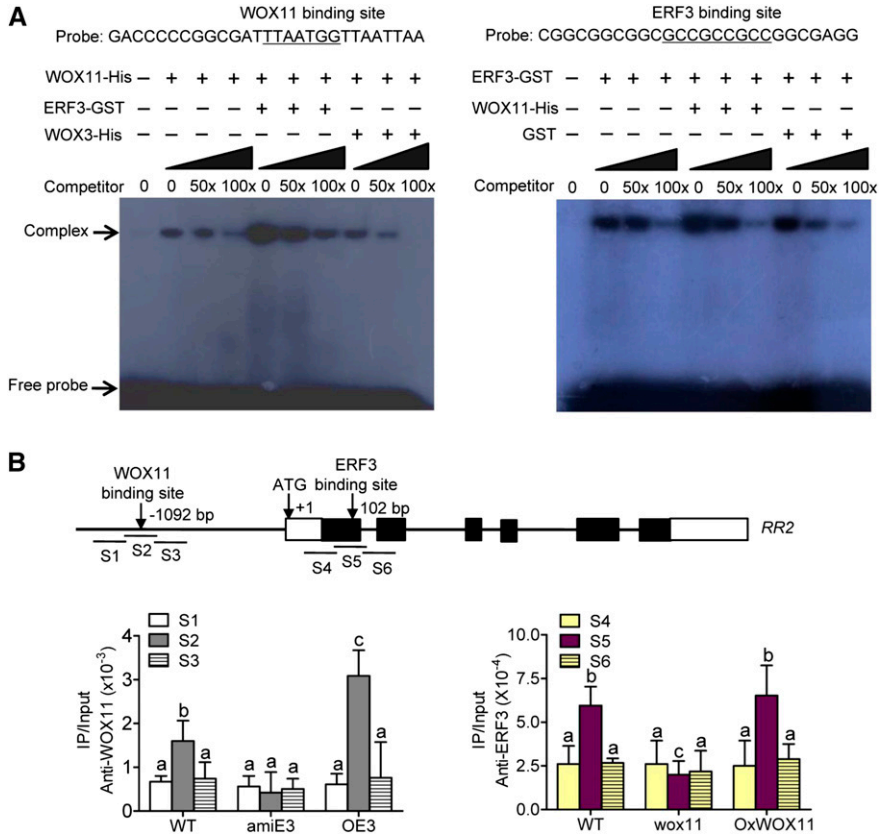

Figure 6. ERF3 Promotes WOX11 Binding to *RR2*.

(A) Gel-shift assays of WOX11 binding to *RR2* promoter containing the WOX11 binding site in the presence or absence of ERF3 (left) and ERF3 binding to *RR2* first exon (P2) containing the ERF binding site in the presence or absence of WOX11 (right). *E. coli*-produced ERF3 and WOX11 proteins were incubated with ^{32}P-labeled probes in the absence or presence of 50 or 100 M excess of the corresponding cold probes and analyzed by electrophoresis. The shifted band is indicated by the arrow. Three biological replicates were conducted.

(B) ChIP analysis of ERF3 and WOX11 binding to *RR2* in different transgenic plants. Nuclei from *OE3*, *amiE3*, *wox11*, *OxWOX11*, and the wild type (WT) were immunoprecipitated by WOX11 (left) or ERF3 (right) antibodies. The precipitated chromatin fragments were analyzed by qPCR using six primer sets amplifying six *RR2* regions (S1, S2, S3, S4, S5, and S6) as indicated. The relative nucleotide positions of the putative WOX11/ERF3 binding sites are indicated with arrows. One-tenth of the input (without antibody precipitation) chromatin was analyzed and used as control. Three biological replications were performed. Each value is the average ± SD from three independent experiments. Significant differences between samples (*t* test) are indicated by different letters.

the expression of *WOX11* (Figure 4A). However, the level of *ERF3* transcripts was decreased in *wox11* (Supplemental Figure 4A), suggesting WOX11 might regulate *ERF3*. To further dissect the genetic relationship of ERF3 and WOX11 in controlling crown root development, we then generated *ERF3* knockdown transgenic lines in the *wox11* mutant background (*amiERF3/wox11*), in which *ERF3* transcript was greatly reduced (Figure 7A). The *amiERF3/wox11* lines displayed a more severe phenotype compared with the *wox11* mutant. Some of the transgenic lines did not produce any primary or crown root during rooting stage (Supplemental Figure 4B), while others had much fewer and shorter crown roots in T1 lines compared with *wox11* (Figure 7B, Table 2). Meanwhile, the transcript levels of *RR2* clearly decreased in *amiERF3/wox11* plants (Figure 7E), indicating an important role for the ERF3 and WOX11 interaction in regulating *RR2* transcription. The more severe phenotype of *amiERF3/wox11* suggested that *WOX11* alone is not sufficient to fully maintain crown root formation in the absence of *ERF3* and the two genes could act together during rice crown root development.

Overexpression of *ERF3* Partially Complemented the *wox11* Root Phenotype

To further examine the above-mentioned interaction hypothesis, we introduced *ERF3* under *ERF3* promoter into *wox11* background (ERF3:*ERF3/wox11*). ERF3:*ERF3/wox11* plants produced more crown roots than *wox11* mutants (Figures 7C and 7D), suggesting that increased *EFR3* expression could partially complement the *wox11* root phenotype. Previous results have shown that *wox11* mutation induced *RR2* expression in elongating crown roots (Zhao et al., 2009). To study whether *EFR3* downregulation and overexpression affected *RR2* expression in *wox11* background, in situ

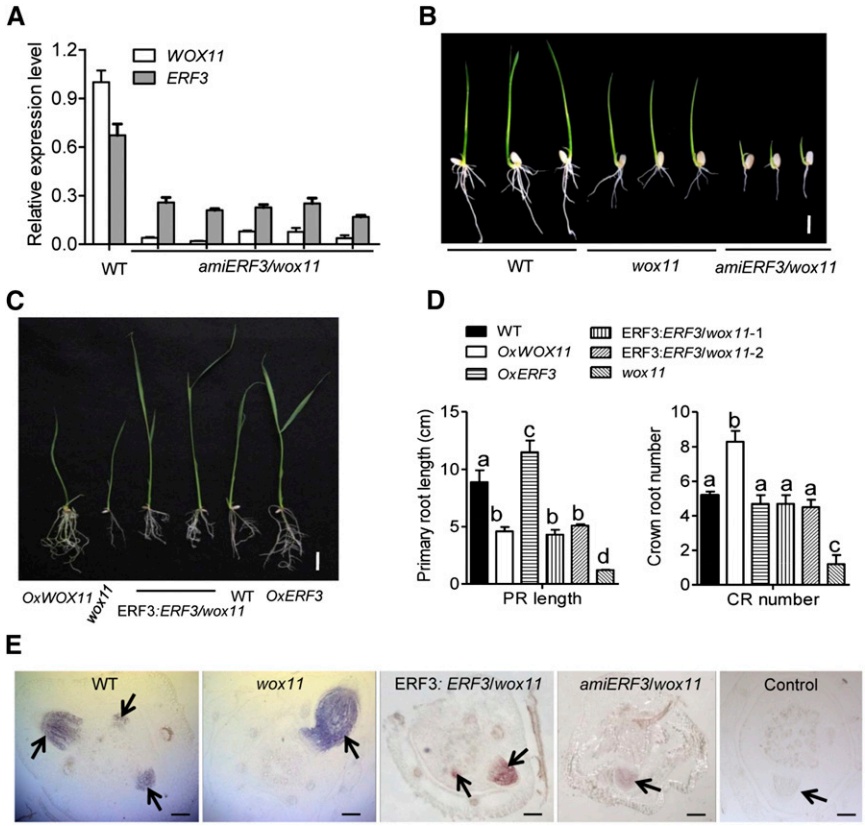

Figure 7. Genetic Relationship between *WOX11* and *ERF3* in Controlling Rice Crown Root Development and *RR2* Expression.

(A) Transcript levels of *ERF3* and *WOX11* in roots of wild-type (WT) and *amiERF3/wox11* plants. The PCR signals were normalized with *ACTIN1* transcripts. Transcript level from the wild type was set at 1. Bars are means ± SD from three technical replicates.

(B) to **(D)** Crown root phenotypes of indicated genotypes. *OxWOX11*, *WOX11* overexpression lines; *OxERF3*, *ERF3* overexpression lines; ERF3:*ERF3/wox11*, *ERF3* cDNA under the *ERF3* promoter in the *wox11* background. Significant differences between samples (*t* test) are indicated by different letters. Bar = 1 cm in **(B)** and 5 cm in **(C)**.

(E) *RR2* transcripts detected by in situ hybridization in the wild type, *wox11*, ERF3:*ERF3/wox11*, and *amiERF3/wox11*. Arrows indicate crown root initials. Bar = 75 μm.

hybridization and RT-qPCR analysis was performed. The analysis revealed that *EFR3* downregulation reduced *RR2* accumulation in elongating crown roots, whereas overexpression of *ERF3* induced *RR2* transcript in crown root initials in *wox11* background (Figure 7E; Supplemental Figure 6A). These data confirmed the function of *ERF3* in regulation of *RR2* expression and suggested that ERF3 was a functional partner of WOX11. The two proteins might play different roles in temporal and spatial expression of *RR2* during crown root initiation and emergence.

RR2 Modulated Root Development by Altered Cytokinin Signaling

To study whether the crown root phenotypes in *ERF3* and *WOX11* transgenic and mutant plants were related to *RR2* expression, we produced *RR2* overexpression (*OxRR2*) and RNAi (*RiRR2*) transgenic plants (Figure 8A). Five overexpression lines (*OxRR2*-1, -14, -27, -31, and -15, among which line 15 is a negative control) and three RNAi lines (*RiRR2*-13, -24, and -26) were selected for detailed phenotypic analysis. The number of crown roots significantly increased in the *OxRR2* lines and reduced in the *RiRR2* lines compared with the wild type (Figure 8B), indicating that the *RR2* expression level was positively correlated with rice crown root initiation. However, both *OxRR2* and *RiRR2* lines showed reduced root lengths compared with the wild type (Table 3), suggesting that the *RR2* expression had a complex effect on root elongation. These results supported the hypothesis that *RR2* expression might be involved in *ERF3/WOX11*-regulated crown root development.

DISCUSSION

ERF3 Participates in Both the Initiation and Elongation Processes during Crown Root Development

Identification and characterization of genes affecting crown root initiation, emergence, and elongation process in rice have contributed to our increasing understanding of the genetic mechanisms

Table 2. Comparison of Primary Root Length and Crown Root Number between the Wild Type, *wox11* Mutants, and *amiERF3/wox11* Transgenic Plants 10 d after Germination

Genotype (Plant Number)	Primary Root Length (cm)	Crown-Borne Root Number
Wild type (16)	2.94 ± 1.68	3.38 ± 0.58
wox11 (14)	1.83 ± 1.22*	2.16 ± 0.27**
amiERF3/wox11 (34)	1.87 ± 1.29*	1.44 ± 0.85**

Significant difference are indicated at the 5% (*) and 1% (**) probability levels (two-tailed *t* test).

underlying crown root development (Inukai et al., 2005; Liu et al., 2005; Kitomi et al., 2008, 2011b; Zhao et al., 2009; Wang et al., 2011). However, it is not clear what these crown root regulators interact with and how the interacting factors regulate crown root formation. In this study, we identified ERF3 as a WOX11-interacting partner in controlling crown root development. ERF3 belongs to the AP2/ERF transcription factor family (Nakano et al., 2006). Other rice AP2/ERF genes, such as *CRL5*, which contains two AP2 repeats, has been shown to regulate crown root initiation as well as other aspects of plant development in rice (Kitomi et al., 2011a). *PLT1* to *PLT6* are all expressed in the primordium of crown root (Li and Xue, 2011). Our data indicate that *ERF3*, which contains one AP2 repeat (Figure 3A), is involved in the control of crown root development likely acting at the initiation, emergence, and elongation steps (Figures 2F, 3C, and 3E, Table 1; Supplemental Figure 2B). Alteration of root meristem sizes in *ERF3* overexpression and knockdown plants suggested that *ERF3* may regulate cell division in root meristem (Figures 3F and 3G). It has been reported that overexpression of *ERF3* (*AP37*) in rice under the control of the constitutive promoter *Cc1* significantly increased grain yield by 16 to 57% over controls under severe drought conditions, yet exhibited no significant difference under normal growth conditions (Oh et al., 2009), which might be at least partially due to the well-developed root system in the plants overexpressing *ERF3*.

ERF3 Promoted Crown Root Development by Mediating Auxin-Cytokinin Signaling Gene Expression

Auxin signaling is required for crown root development, including crown root initiation and emergence. Exogenous auxin application increased crown roots number in rice seedlings (Inukai et al., 2005). Cytokinin also influences lateral root formation by disrupting lateral root initiation and patterning in Arabidopsis (Laplaze et al., 2007; Benková and Hejátko, 2009; Péret et al., 2009). Auxin-cytokinin crosstalk signaling plays key roles in root development and can coordinately regulate a series of genes (Dello Ioio et al., 2008; Müller and Sheen, 2008; Perilli et al., 2013). For example, transcription of root-specific putative homeobox genes *ATHB53* and *WOX11* are differentially regulated by auxin and cytokinin in Arabidopsis and rice, respectively (Son et al., 2005; Zhao et al., 2009). Our data show that auxin and cytokinin could rapidly but transiently induce *ERF3* expression (Figures 2B and 2C) and that overexpression or knockdown of *ERF3* either activated or repressed some auxin- and cytokinin-responsive genes (Figure 4B). Similarly, exogenously supplied auxin (indole3-acetic acid [IAA]) and cytokinin (6-BA) could rescue root phenotypes of *amiERF3* plants (Supplemental Figure 5). These data suggested that *ERF3* might be an auxin-cytokinin-responsive gene and the effect of exogenous hormones on crown root development might be partially mediated by elevation of *ERF3* expression.

In Arabidopsis, disruption of eight of the 10 type-A *ARR* genes affected root development via altering the size of the apical meristem (Zhang et al., 2011). Mutation of a maize type-A *RR* gene, *ABPHL1* (*ABPH1*), induced an increased root meristem size (Giulini et al., 2004). In rice, overexpression of *RR3*, *RR5*, and *RR6* affected crown root development (Hirose et al., 2007; Cheng et al., 2010). *RR2* is directly repressed by WOX11 during crown root development (Zhao et al., 2009). Recent work reported that *RR1* regulates crown root initiation under the control of *CRL5* (Kitomi et al., 2011a). These observations suggest that type-A *RR* genes, which negatively regulate cytokinin signaling, may play important roles in plant root development. The current study indicated that ERF3 directly targets *RR2* and upregulates its expression during crown root initiation (Figures 4C, 5B, and 5C). Furthermore, the data showing that *RR2* overexpression augmented crown root numbers and its knockdown had an opposite effect (Figure 8), which indicated that *RR2* is a bona fide downstream target of ERF3 involved in crown root initiation. Taken together, these results suggested that activation of type-A *RR2* gene by ERF3, which

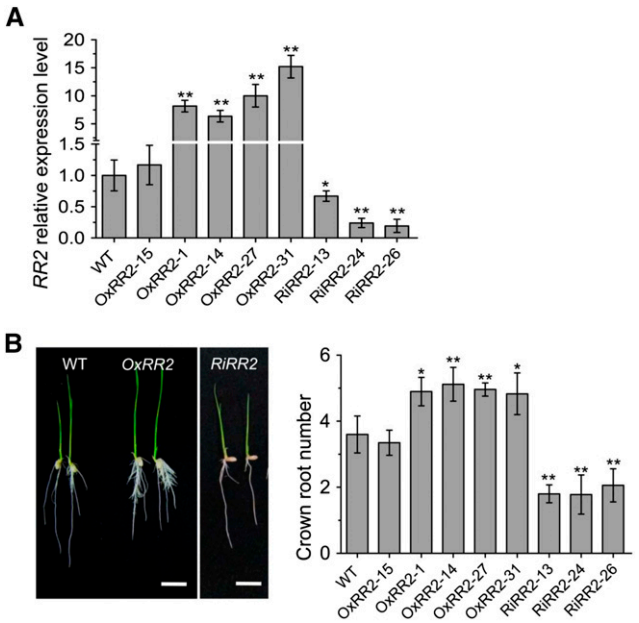

Figure 8. Root Phenotypes of *RR2* Overexpression and RNAi Transgenic Plants.

(A) Relative *RR2* transcript levels in the wild type (set as 1), five *RR2* overexpression (*OxRR2*), and three *RR2* RNAi lines (*RiRR2*). The PCR signals were normalized with *ACTIN1* transcripts. Transcript level from the wild type was set at 1. Error bars represent SD. *P < 0.05 and **P < 0.01.
(B) Root phenotype of *RR2* overexpression (*OxRR2*), three RNAi (*RiRR2*) transgenic plants, and the wild type (WT). Statistical analyses of the data are presented in Table 3. Bars = 1 cm.

Table 3. Comparison of Primary Root Length between the Wild Type, *RR2* Overexpressing (*OxRR2*), and RNAi Transgenic Lines (*RiRR2*) 10 d after Germination

Genotype (Plant Number)	Primary Root Length (cm)
Wild type (20)	6.01 ± 0.55
OxRR2-15 (16)	6.48 ± 0.71
OxRR2-1 (16)	4.66 ± 0.55**
OxRR2-14 (15)	4.59 ± 0.78**
OxRR2-27 (15)	4.36 ± 0.64**
OxRR2-31 (17)	4.82 ± 0.81**
RiRR2-13 (15)	3.48 ± 0.59**
RiRR2-24 (14)	3.94 ± 0.63**
RiRR2-26 (15)	3.41 ± 0.67**

Significant differences are indicated at the 5% (*) and 1% (**) probability levels (two-tailed *t* test). *OxRR2*-15 is a negative control.

might repress cytokinin signaling in crown root initials, enhanced root meristem activity and promoted crown root formation.

The Gene Regulatory Pathway Controlling Crown Root Development in Rice

In rice, WOX11 is a key regulator in crown root development (Zhao et al., 2009). Thus far, the regulatory network by which WOX11 regulates downstream targets is unknown. This work identified ERF3 as an interacting partner of WOX11 (Figure 1). However, *ERF3* transcripts were detectable in crown root initials and in emerging crown root meristem (Figures 2D to 2H), whereas *WOX11* is expressed mostly in the active cell division region of the emerging crown root meristem (Zhao et al., 2009). This suggested that the expression pattern of *ERF3* only partially overlapped with that of *WOX11* during crown root development (Figure 2F; Zhao et al., 2009), and interaction between ERF3 and WOX11 most likely occurred after crown root emergence. Previous work showed that WOX11 represses *RR2* in elongating crown roots (Zhao et al., 2009).

The observations that *RR2* mRNA levels was higher in crown root initials and gradually decreased during crown root growth (Zhao et al., 2009), suggesting that ERF3 and WOX11 might contribute to the spatial and temporal expression pattern of *RR2* (Figure 9A). Because the WOX11/ERF3 interaction enhanced WOX11 binding to the *RR2* promoter (Figure 6), and in *amiERF3/wox11* roots, *RR2* expression was even lower than in the wild type (Supplemental Figure 6), we speculated that in the elongating crown root meristem, the WOX11/ERF3 interaction might either enhance WOX11-mediated repression or inhibit ERF3-mediated activation of *RR2*.

Based on our data, we proposed a model of the regulatory pathway controlling crown root development in rice (Figure 9B). In crown root initials, ERF3 directly binds to *RR2* and upregulates its expression, resulting in repression of cytokinin signaling and promotion of crown root initiation. In emerging crown roots, *WOX11* expression was turned on and its binding to *RR2* was enhanced by interaction with ERF3, leading to inhibition of ERF3 function or direct repression of *RR2* and enhanced cytokinin signaling that promotes crown root elongation.

The *CRL1/ARL1-CRL5* pathways affect crown root initiation by auxin (Inukai et al., 2005; Liu et al., 2005; Kitomi et al., 2011a). However, the expression of *WOX11* is not regulated by *CRL5* (Kitomi et al., 2011a). In this study, we found that *CRL5* expression was unlikely to be regulated directly by *ERF3* (Figure 4A). These results suggested that the crown root development pathway regulated by ERF3 and WOX11 might differ from the pathway regulated by *CRL1/ARL1-CRL5*. Further studies are needed to identify the interrelationship between these pathways in order to further understand the molecular regulatory mechanism of crown root development in rice.

Collectively, our data suggested a spatio-temporal sequence of events that may act in cytokinin signaling from crown root initiation to crown root elongation. This sequence involved a shift of *RR2* activation toward *RR2* repression, which linked to spatial expression of *WOX11* and *ERF3*. Through the downstream effect on *RR2* expression, this regulatory module determines the spatial frame for crown root initiation and consequently for crown root

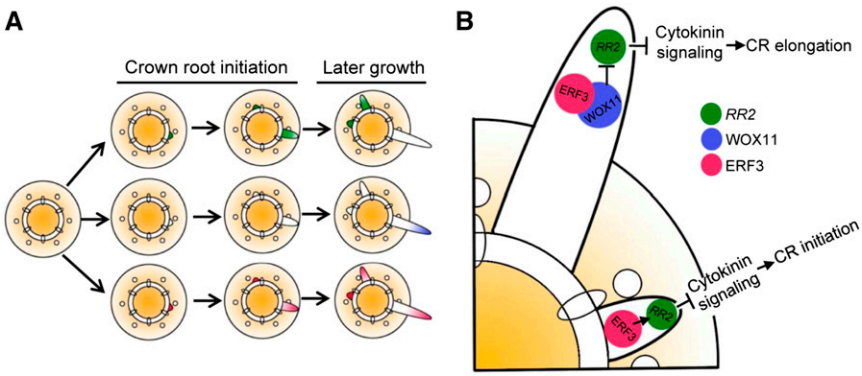

Figure 9. Proposed Models for *ERF3*, *WOX11*, and *RR2* Expression Patterns and Their Functions in Controlling Crown Root Initiation and Elongation in Rice.

(A) Model of *ERF3*, *WOX11*, and *RR2* expression patterns during crown root formation.

(B) Model of *ERF3*, *WOX11*, and *RR2* functions controlling crown root initiation and elongation in rice.

During crown root initiation, *ERF3* repressed cytokinin signaling by directly activating *RR2* expression. During crown root elongation, *WOX11* expression was turned on. WOX11-ERF3 interaction either enhances WOX11-mediated repression or inhibits ERF3-mediated activation of *RR2*, leading to cytokinin signaling activation and thereby promoting crown root growth.

elongation. In conclusion, our discoveries revealed a regulatory mechanism underlying rice crown root development, which greatly advanced our understanding of adventitious root formation in crop plants, which appears to differ substantially from that in Arabidopsis. Thus, our work provided a foundation for further understanding crown root organogenesis and for crop improvement via targeting the ERF3/WOX11 pathway.

METHODS

Plant Materials and Growth Conditions

The rice variety Zhonghua11 (ZH11) (*Oryza sativa* subsp *japonica*) was used for transformation in this study. The *wox11* mutant previously reported by Zhao et al. (2009) was introduced into the ZH11 background by backcrosses. All transgenic plants were produced in the ZH11 background, genotyped by PCR in the T2 segregating populations. Multiple independent segregating lines were used for molecular and phenotypic analysis. For in vitro cultures, rice seeds were surface-sterilized and germinated in media containing 0.8% agar supplemented with 3% (w/v) sucrose at 28°C (in light) and 24°C (in dark) with a 14-h-light/10-h-dark cycle or in fields.

Yeast Two-Hybrid Screening

The ProQuest system (Invitrogen) was used to screen for WOX11-interacting proteins following the manufacturer's protocol. Briefly, a construct that contains the *WOX11* full-length cDNA was cloned by PCR into the *Sal*I and *Spe*I sites of Proquest's pDBleu vector, and a rice cDNA library was built into the expression vector pEXP-AD502 of the ProQuest system using the restriction enzymes *Not*I and *Sal*I with mRNA isolated from roots of ZH11 plants with two tillers. Total RNA was isolated using Trizol reagent (Invitrogen), and mRNA was then purified using the Absolutely mRNA purification kit (Stratagene) according to the protocol provided by the manufacturer. The primers WOX11-2YH F/R used in PCR amplification are listed in Supplemental Table 1.

In Vitro Pull-Down Assay

Pull-down was performed as described (Yang et al., 2008) with the following modifications: Equal volumes of GST or WOX3-His, and ERF3-GST or WOX11-His recombinant proteins were incubated for 6 h at 4°C with 400 μL of GST (GE Healthcare; 17-5132-01) or His (Promega; REF V8500) resin in a total volume of 1 mL of GST or His binding buffer (20 mM Tris-HCl, pH 8.0, 200 mM NaCl, 1 mM EDTA, 0.5% Lgepal CA-630, and protease inhibitor) for 2 to 3 h at 4°C, and the binding reaction was washed five times (10 min each time at 4°C) by the binding buffer. After extensive washing, the pulled down proteins were eluted by boiling, separated on 12% SDS-PAGE, and detected by immunoblots using an anti-GST antibody (abcam; ab19256) and anti-His antibody (abcam; ab9108), respectively.

Coimmunoprecipitation Assay

Coimmunoprecipitation assays were performed as previous described (Sun and Zhou, 2008). Total nuclear protein from roots of 10-d transformed plants and wild-type seedlings was extracted and ground in liquid nitrogen. Total nuclear proteins were extracted in nuclear extraction buffer 1 (2 mM EDTA, 2.5 mM DTT, 10 mM HEPES, pH 8.0, and 0.4 M sucrose) containing protease inhibitor cocktail (Roche). Cell debris was collected by centrifugation at 3000*g* for 10 min at 4°C and suspended with Nuclear Extraction Buffer 2 (10 mM $MgCl_2$, 10 mM HEPES, pH 8.0, and 2.5 M sucrose containing protease inhibitor cocktail [Roche]), Nuclear Extraction Buffer 3, and coimmunoprecipitation buffer, respectively. The supernatant was incubated with anti-WOX11 (see below) or anti-FLAG (Sigma-Aldrich; F3165) specific antibody overnight at 4°C by gentle rotation. Then, 60 μL of protein G agarose beads (Millipore) was added. After 2 to 3 h of incubation at 4°C with gentle rotation, the beads were centrifuged and washed three times with 600 μL washing buffer (100 mM Tris-HCl, pH 7.4, 75 mM NaCl, 1 mM EDTA, 10% glycerol, 0.05% SDS, 0.1% Triton X-100, and protease inhibitor cocktail). FLAG proteins were eluted under acidic conditions and analyzed by immunoblots using anti-FLAG and anti-WOX11 antibodies.

The peptide-affinity polyclonal antibody against WOX11 (amino acids 177 to 191) was raised by Neweast Biotechnology. The specificity of this purified antibody was confirmed by immunoblot.

BiFC and Fluorescence Microscopy

BiFC assays were performed as described previously (Waadt et al., 2008). For generation of the BiFC vectors, the full-length cDNA of *ERF3* was amplified with primer pairs ERF3BiFC-F/ R (Supplemental Table 1) and cloned at the *Spe*I-*Kpn*I sites in pVYCE(R). The full-length cDNA of *WOX11* was cloned into the *Spe*I-*Kpn*I sites of pVYNE(R). Rice mesophyll protoplasts were prepared and the two fusion proteins were transiently co-transfected into rice protoplasts with Ghd7:CFP, as described (Zhou et al., 2009), with minor modifications. Fluorescence in the transformed protoplasts was imaged using a confocal laser scanning microscope (TCS SP2; Leica) after incubation at 23°C for 12 to18 h.

Vector Construction and Rice Transformation

For the construction of the fusion between the *ERF3* promoter and the GUS coding sequence, the 2.561-kb *ERF3* promoter was amplified from ZH11 genomic DNA by primer set ERF3pgus-F/R and inserted into pCAMBIA1381Xb (CAMBIA) at the *Bam*HI and *Sal*I sites.

To analyze the function of *ERF3*, the amiRNA strategy was used to knock down the *ERF3* gene (Ossowski et al., 2008). For amiRNAs of the *ERF3* construct, the 250-bp fragment containing 21-mers recognizing specifically the 39 untranslated region of *ERF3* transcripts was amplified using universal primers G11491/G11494 and specific primers, including ERF3miR-s, ERF3miR-a, ERF3miR-*s, and ERF3miR-*a, which were designed in WMD2 (http://wmd3.weigelworld.org/cgi-bin/webapp.cgi) as described previously (Warthmann et al., 2008), and then cloned into *Kpn*I-*Bam*HI-digested pU1301 (Chu et al., 2006).

For overexpression and ERF3-FLAG fusion constructs, the full-length cDNA of *ERF3* amplified with the primer set ERF3ox-F/R and ERF3flag-F/R was inserted into the *Kpn*I and *Bam*HI sites of pU1301 and pU2301, respectively (Dai et al., 2007; Sun and Zhou, 2008).

To construct the *RR2* overexpression and RNAi vector, the full-length cDNA and a specific cDNA fragment of *RR2* were amplified using the primer set OxRR2F/R and RiRR2-F/R and inserted into pU1301 and pDS1301 vectors, respectively (Chu et al., 2006; Dai et al., 2007).

All constructs were introduced into ZH11 plants by *Agrobacterium tumefaciens* (EHA105)-mediated transformation as previously described (Dai et al., 2007). All primers for genotyping and vector construction are listed in Supplemental Table 1.

In Situ Hybridization

The hybridization and immunological detection were performed as described by Zhao et al. (2009). The *ERF3* probe was amplified using the gene-specific primers ERF3situ-F/R (Supplemental Table 1). The PCR fragment was inserted into the *Spe*I and *Bam*HI sites of pGEM-T (Promega) and transcribed in vitro from either the T7 or SP6 promoter for sense or antisense strand synthesis using the Digoxigenin RNA labeling kit (Roche). The *RR2* probe was previously described (Zhao et al., 2009).

Promoter Activity Detection and Histological Observation

Roots of Pro_{OsERF3}-GUS transgenic plants harvested 14 d after germination were incubated with X-gluc buffer overnight at 37°C (Jefferson et al., 1987) and directly photographed. Roots and the coleoptilar nodal region of different *ERF3* transgenic lines and the wild type were fixed with 50% FAA (formalin/acetic acid/alcohol) at 4°C overnight. The staining and dehydration were performed according to the previously described method (Liu et al., 2005) and embedded with cold-curing resin (Heraeus Kulzer Dental) using the Technovit 7100 system. The microtome sections (4-μm thickness) were mounted on glass slides and stained with 0.25% toluidine blue. Sections were observed under a bright-field microscope (Zeiss AxioCam HRC) and photographed with a differential interference microscope (Nikon 80i). Root length was measured with Image J software (http://rsb.info.nih.gov/ij). Root meristem size was determined by measuring the length from the quiescent center to the first elongated epidermal cell. The average cell length in the root meristem was quantified with cells (as shown with red lines in the figures). For each quantification, at least 15 rice plants were analyzed.

EMSA

To produce the ERF3 protein, the full-length cDNA amplified with primers ERF3protein-F/R was inserted into the *Bam*HI and *Sal*I sites of the pGEX-4T-1 expression vector (GE Healthcare) and expressed in *Escherichia coli* DE3 (BL21) cells (GE Healthcare). The target protein was purified with GST four fast flow (GE Healthcare). The *RR2* promoter DNA P1 (including the putative ERE binding site GCCGCC), 1st exon DNA P2 (including the putative ERE binding site GCCGCCGCC), P2 deletion (with nucleotide deletions in the ERE binding site), and 1st intron DNA P3 (including GCCGCC) were produced by annealing of oligonucleotides EMSAp1-F/R, EMSAp2-F/R, EMSAp2d-F/-R, and EMSAp3-F/R, respectively. The double-stranded oligonucleotides EMSAp1, EMSAp2, EMSAp2d, and EMSAp3 were labeled with [^{32}P]dCTP using a Klenow fragment. DNA binding reactions were performed in the presence or absence of unlabeled P1, P2, P2d, and P3 fragments at different molar excess at room temperature for 20 min in 10 mM Tris, pH 7.5, 50 mM NaCl, 1 mM DTT, 1 mM EDTA, 1 mM $MgCl_2$, 5% glycerol, and 50 mg/L poly(dI-dC) (Amersham Pharmacia Biotech). The reactions were resolved on 6% polyacrylamide gels in Tris-glycine (0.3% Tris and 1.88% glycine) buffer and visualized by autoradiography. The sequences of the primers used are listed in Supplemental Table 1.

In Vivo Binding Assay of ERF3 and WOX11 by ChIP

For ChIP assays, wild-type and *ERF3*-FLAG transgenic lines were used for chromatin extraction and immunoprecipitation as described by Huang et al. (2007). Briefly, roots were treated with formaldehyde and the nuclei were isolated and sonicated using an Ultrasonic Crasher Noise Isolating Chamber (Scientz). The soluble chromatin fragments were isolated and preabsorbed with sheared salmon sperm DNA/protein A-agarose (Sigma-Aldrich) to remove nonspecific binding. Immunoprecipitations with anti-FLAG (Sigma-Aldrich; F3165) or without any serum were performed as described. The precipitated DNA was analyzed by qPCR using specific primer sets ERF3ChIPs4F/R, ERF3ChIPs5F/R, and ERF3ChIPs6F/R (Supplemental Table 1). *WOX11* ChIP qPCR primers are described in (Zhao et al., 2009). Typically, the precipitated and input DNA samples were analyzed by qPCR with gene-specific primers listed in Supplemental Table 1. Data normalized with input transcripts are means from three biological repeats ± SD. The values from nontreated samples were assessed as 1.

RT-qPCR

Total RNA was isolated using TRIzol reagent and reverse-transcribed according to the manufacturer's instructions (Invitrogen). RT-qPCR was performed using gene-specific primers (Supplemental Table 1) and SYBR Premix Ex Taq on a real-time PCR 7500 system (Applied Biosystems). Data were collected using the ABI PRISM 7500 sequence detection system following the instruction manual. The rice *ACTIN1* gene was used as the internal control. At least three biological replicates and three technical repeats were tested.

RNA Gel Blot and Immunoblot

For RNA gel-blotting analysis, 15 μg of total RNA samples extracted from tissues or organs harvested from field-grown rice plants was separated in 1.2% (w/v) formamide-denaturing agarose gels, before being transferred to nylon membranes. Gene-specific probes were labeled with [^{32}P]dCTP using the Random Primer kit (Invitrogen) and hybridized to the RNA gel blots. The probe for *ERF3* was digested from T/A plasmid with *Kpn*I and *Bam*HI, a fragment of 635 bp of the cDNA.

Rice root nuclear protein was extracted from wild-type and ERF3-FLAG transgenic plants and performed as described previously (Tariq et al., 2003). After being washed in acetone and dried, the proteins were resuspended in Laemmli sample buffer (62.5 mM Tris-HCl, pH 6.8, 2% SDS, 25% glycerol, 0.01% bromophenol blue, and 10% β-mercaptoethanol), then separated by 16% SDS-PAGE and transferred to an Immobilon-P polyvinylidene fluoride transfer membrane (Millipore). The membrane was blocked with 2% BSA in PBS (pH 7.5) and incubated overnight with primary antibodies, such as anti-FLAG (F3165; Sigma-Aldrich), in a 1:5000 dilution at 4°C. After three washes (30 min each), the secondary antibody (goat anti-mouse IgG [SouthernBiotech]) at 1:10,000 dilution was used. Visualization was performed using the Super Signal West Pico kit (Pierce) according to the manufacturer's instructions.

Exogenous IAA, Naphthalene Acetic Acid, and 6-BA Treatment

Seeds were sown and germinated on agar medium. After 10 d, the seedlings were transferred to media with or without 10^{-6} M 2,4-D, or 10^{-5} M 6-BA. Total RNA was extracted after 0, 0.5, 1, 3, 4, 6, 9, and 12 h of treatment and analyzed by RT-qPCR with primers ERF3qPCR-F/R. For root growth tests, transgenic plants and wild-type seeds were germinated on agar medium containing 10^{-6} M 2,4-D, 10^{-6} M IAA, or 10^{-5} M 6-BA. Ten days after treatment, crown root phenotypes were recorded.

Accession Numbers

Sequence data from this article can be found in the GenBank/EMBL databases under the following accession numbers: *ERF3*, AK061380, LOC_Os01g58420; *CRL1*, AK064187 LOC_03g05510; *CRL4*, AK240747, LOC_Os03g46330; and *CRL5*, AK109848, LOC_Os07g03250. The accession numbers of other genes can be found in Zhao et al. (2009).

Supplemental Data

Supplemental Figure 1. Detection of *ERF3* mRNA and protein in ERF3-FLAG transgenic and wild-type plants by RNA gel blot and immunoblot.

Supplemental Figure 2. Cell longitudinal length in root meristem zone and crown root primordium number in *ERF3* transgenic plants and wild-type seedlings.

Supplemental Figure 3. Gel shift assay of ERF3 protein binding to P1, P2, and P3 regions of *RR2* containing the ERF binding sites (underlined).

Supplemental Figure 4. Detection of expression level of *ERF3* in wild type and *wox11* and phenotype of crown root of *amiERF3/wox11* transgenic plants at rooting stage.

Supplemental Figure 5. Auxin (2,4-D and IAA) and cytokinin (6-BA) rescued the root phenotype of ERF3 artificial microRNA (*amiE3*) transgenic plants.

Supplemental Figure 6. RT-qPCR and in situ hybridization detection of *RR2* expression in *wox11*, ERF3:*ERF3wox11*, *amiERF3wox11*, and wild-type roots.

Supplemental Table 1. Primers used in this study.

ACKNOWLEDGMENTS

We thank Qinglu Zhang and Xianghua Li for help in field experiments and management. This research was supported by grants from the National Natural Science Foundation of China (31371468), the Program for New Century Excellent Talents in University (NCET-12-0863), and the Fundamental Research Funds for the Central Universities (2013PY021).

AUTHOR CONTRIBUTIONS

Y.Z., D.-X.Z., and S.C. designed the research and analyzed the experimental data. S.C., Y.Z., Y.S., Y.H., and S.Z. performed the experiments. Y.Z. and D.-X.Z. wrote the article.

Received March 16, 2015; revised August 3, 2015; accepted August 9, 2015; published August 25, 2015.

REFERENCES

Benková, E., and Hejátko, J. (2009). Hormone interactions at the root apical meristem. Plant Mol. Biol. **69:** 383–396.

Bishopp, A., Help, H., and Helariutta, Y. (2009). Cytokinin signaling during root development. Int. Rev. Cell Mol. Biol. **276:** 1–48.

Cheng, X., Jiang, H., Zhang, J., Qian, Y., Zhu, S., and Cheng, B. (2010). Overexpression of type-A rice response regulators, OsRR3 and OsRR5, results in lower sensitivity to cytokinins. Genet. Mol. Res. **9:** 348–359.

Chu, Z., Yuan, M., Yao, J., Ge, X., Yuan, B., Xu, C., Li, X., Fu, B., Li, Z., Bennetzen, J.L., Zhang, Q., and Wang, S. (2006). Promoter mutations of an essential gene for pollen development result in disease resistance in rice. Genes Dev. **20:** 1250–1255.

Coudert, Y., Périn, C., Courtois, B., Khong, N.G., and Gantet, P. (2010). Genetic control of root development in rice, the model cereal. Trends Plant Sci. **15:** 219–226.

Dai, M., Hu, Y., Zhao, Y., Liu, H., and Zhou, D.X. (2007). A WUSCHEL-LIKE HOMEOBOX gene represses a YABBY gene expression required for rice leaf development. Plant Physiol. **144:** 380–390.

Dello Ioio, R., Linhares, F.S., and Sabatini, S. (2008). Emerging role of cytokinin as a regulator of cellular differentiation. Curr. Opin. Plant Biol. **11:** 23–27.

Dello Ioio, R., Linhares, F.S., Scacchi, E., Casamitjana-Martinez, E., Heidstra, R., Costantino, P., and Sabatini, S. (2007). Cytokinins determine Arabidopsis root-meristem size by controlling cell differentiation. Curr. Biol. **17:** 678–682.

De Smet, I., and Jürgens, G. (2007). Patterning the axis in plants–auxin in control. Curr. Opin. Genet. Dev. **17:** 337–343.

Du, L., Jiao, F., Chu, J., Jin, G., Chen, M., and Wu, P. (2007). The two-component signal system in rice (*Oryza sativa* L.): a genome-wide study of cytokinin signal perception and transduction. Genomics **89:** 697–707.

Durbak, A., Yao, H., and McSteen, P. (2012). Hormone signaling in plant development. Curr. Opin. Plant Biol. **15:** 92–96.

Gao, S., Fang, J., Xu, F., Wang, W., Sun, X., Chu, J., Cai, B., Feng, Y., and Chu, C. (2014). CYTOKININ OXIDASE/DEHYDROGENASE4 integrates cytokinin and auxin signaling to control rice crown root formation. Plant Physiol. **165:** 1035–1046.

Giulini, A., Wang, J., and Jackson, D. (2004). Control of phyllotaxy by the cytokinin-inducible response regulator homologue ABPHYL1. Nature **430:** 1031–1034.

Goh, T., Joi, S., Mimura, T., and Fukaki, H. (2012). The establishment of asymmetry in Arabidopsis lateral root founder cells is regulated by LBD16/ASL18 and related LBD/ASL proteins. Development **139:** 883–893.

Hao, D., Ohme-Takagi, M., and Sarai, A. (1998). Unique mode of GCC box recognition by the DNA-binding domain of ethylene-responsive element-binding factor (ERF domain) in plant. J. Biol. Chem. **273:** 26857–26861.

Hirose, N., Makita, N., Kojima, M., Kamada-Nobusada, T., and Sakakibara, H. (2007). Overexpression of a type-A response regulator alters rice morphology and cytokinin metabolism. Plant Cell Physiol. **48:** 523–539.

Huang, L., Sun, Q., Qin, F., Li, C., Zhao, Y., and Zhou, D.X. (2007). Down-regulation of a SILENT INFORMATION REGULATOR2-related histone deacetylase gene, OsSRT1, induces DNA fragmentation and cell death in rice. Plant Physiol. **144:** 1508–1519.

Inukai, Y., Sakamoto, T., Ueguchi-Tanaka, M., Shibata, Y., Gomi, K., Umemura, I., Hasegawa, Y., Ashikari, M., Kitano, H., and Matsuoka, M. (2005). Crown rootless1, which is essential for crown root formation in rice, is a target of an AUXIN RESPONSE FACTOR in auxin signaling. Plant Cell **17:** 1387–1396.

Itoh, J., Nonomura, K., Ikeda, K., Yamaki, S., Inukai, Y., Yamagishi, H., Kitano, H., and Nagato, Y. (2005). Rice plant development: from zygote to spikelet. Plant Cell Physiol. **46:** 23–47.

Jain, M., Kaur, N., Garg, R., Thakur, J.K., Tyagi, A.K., and Khurana, J.P. (2006). Structure and expression analysis of early auxin-responsive Aux/IAA gene family in rice (*Oryza sativa*). Funct. Integr. Genomics **6:** 47–59.

Jefferson, R.A., Kavanagh, T.A., and Bevan, M.W. (1987). GUS fusions: beta-glucuronidase as a sensitive and versatile gene fusion marker in higher plants. EMBO J. **6:** 3901–3907.

Kitomi, Y., Ito, H., Hobo, T., Aya, K., Kitano, H., and Inukai, Y. (2011a). The auxin responsive AP2/ERF transcription factor CROWN ROOTLESS5 is involved in crown root initiation in rice through the induction of OsRR1, a type-A response regulator of cytokinin signaling. Plant J. **67:** 472–484.

Kitomi, Y., Kitano, H., and Inukai, Y. (2011b). Molecular mechanism of crown root initiation and the different mechanisms between crown root and radicle in rice. Plant Signal. Behav. **6:** 1270–1278.

Kitomi, Y., Ogawa, A., Kitano, H., and Inukai, Y. (2008). CRL4 regulates crown root formation through auxin transport in rice. Plant Root **2:** 19–28.

Laplaze, L., et al. (2007). Cytokinins act directly on lateral root founder cells to inhibit root initiation. Plant Cell **19:** 3889–3900.

Lee, H.W., Kim, N.Y., Lee, D.J., and Kim, J. (2009). LBD18/ASL20 regulates lateral root formation in combination with LBD16/ASL18 downstream of ARF7 and ARF19 in Arabidopsis. Plant Physiol. **151:** 1377–1389.

Lee, Y., Lee, W.S., and Kim, S.H. (2013). Hormonal regulation of stem cell maintenance in roots. J. Exp. Bot. **64:** 1153–1165.

Li, P., and Xue, H. (2011). Structural characterization and expression pattern analysis of the rice PLT gene family. Acta Biochim. Biophys. Sin. (Shanghai) **43:** 688–697.

Liu, H., Wang, S., Yu, X., Yu, J., He, X., Zhang, S., Shou, H., and Wu, P. (2005). ARL1, a LOB-domain protein required for adventitious root formation in rice. Plant J. **43:** 47–56.

Liu, S., Wang, J., Wang, L., Wang, X., Xue, Y., Wu, P., and Shou, H. (2009). Adventitious root formation in rice requires OsGNOM1 and is mediated by the OsPINs family. Cell Res. **19:** 1110–1119.

Müller, B., and Sheen, J. (2008). Cytokinin and auxin interaction in root stem-cell specification during early embryogenesis. Nature **453:** 1094–1097.

Marcon, C., Paschold, A., and Hochholdinger, F. (2013). Genetic control of root organogenesis in cereals. Methods Mol. Biol. **959:** 69–81.

Moubayidin, L., Perilli, S., Dello Ioio, R., Di Mambro, R., Costantino, P., and Sabatini, S. (2010). The rate of cell differentiation controls the Arabidopsis root meristem growth phase. Curr. Biol. **20:** 1138–1143.

Nakamura, A., Umemura, I., Gomi, K., Hasegawa, Y., Kitano, H., Sazuka, T., and Matsuoka, M. (2006). Production and characterization of auxin-insensitive rice by overexpression of a mutagenized rice IAA protein. Plant J. **46:** 297–306.

Nakano, T., Suzuki, K., Fujimura, T., and Shinshi, H. (2006). Genome-wide analysis of the ERF gene family in Arabidopsis and rice. Plant Physiol. **140:** 411–432.

Oh, S.J., Kim, Y.S., Kwon, C.W., Park, H.K., Jeong, J.S., and Kim, J.K. (2009). Overexpression of the transcription factor AP37 in rice improves grain yield under drought conditions. Plant Physiol. **150:** 1368–1379.

Okushima, Y., Fukaki, H., Onoda, M., Theologis, A., and Tasaka, M. (2007). ARF7 and ARF19 regulate lateral root formation via direct activation of LBD/ASL genes in Arabidopsis. Plant Cell **19:** 118–130.

Ossowski, S., Schwab, R., and Weigel, D. (2008). Gene silencing in plants using artificial microRNAs and other small RNAs. Plant J. **53:** 674–690.

Péret, B., De Rybel, B., Casimiro, I., Benková, E., Swarup, R., Laplaze, L., Beeckman, T., and Bennett, M.J. (2009). Arabidopsis lateral root development: an emerging story. Trends Plant Sci. **14:** 399–408.

Perilli, S., Perez-Perez, J.M., Di Mambro, R., Peris, C.L., Díaz-Triviño, S., Del Bianco, M., Pierdonati, E., Moubayidin, L., Cruz-Ramírez, A., Costantino, P., Scheres, B., and Sabatini, S. (2013). RETINOBLASTOMA-RELATED protein stimulates cell differentiation in the Arabidopsis root meristem by interacting with cytokinin signaling. Plant Cell **25:** 4469–4478.

Ruzicka, K., Simásková, M., Duclercq, J., Petrásek, J., Zazímalová, E., Simon, S., Friml, J., Van Montagu, M.C.E., and Benková, E. (2009). Cytokinin regulates root meristem activity via modulation of the polar auxin transport. Proc. Natl. Acad. Sci. USA **106:** 4284–4289.

Scheres, B. (2002). Plant patterning: TRY to inhibit your neighbors. Curr. Biol. **12:** R804–R806.

Schiefelbein, J. (2003). Cell-fate specification in the epidermis: a common patterning mechanism in the root and shoot. Curr. Opin. Plant Biol. **6:** 74–78.

Son, O., et al. (2005). Induction of a homeodomain-leucine zipper gene by auxin is inhibited by cytokinin in Arabidopsis roots. Biochem. Biophys. Res. Commun. **326:** 203–209.

Su, Y.H., Liu, Y.B., and Zhang, X.S. (2011). Auxin-cytokinin interaction regulates meristem development. Mol. Plant **4:** 616–625.

Sun, Q., and Zhou, D.X. (2008). Rice jmjC domain-containing gene JMJ706 encodes H3K9 demethylase required for floral organ development. Proc. Natl. Acad. Sci. USA **105:** 13679–13684.

Tariq, M., Saze, H., Probst, A.V., Lichota, J., Habu, Y., and Paszkowski, J. (2003). Erasure of CpG methylation in Arabidopsis alters patterns of histone H3 methylation in heterochromatin. Proc. Natl. Acad. Sci. USA **100:** 8823–8827.

Verstraeten, I., Beeckman, T., and Geelen, D. (2013). Adventitious root induction in *Arabidopsis thaliana* as a model for in vitro root organogenesis. Methods Mol. Biol. **959:** 159–175.

Waadt, R., Schmidt, L.K., Lohse, M., Hashimoto, K., Bock, and R., Kudla, J. (2008). Multicolor bimolecular fluorescence complementation reveals simultaneous formation of alternative CBL/CIPK complexes in planta. Plant J. **56:** 505–516.

Wang, S., Xu, Y., Li, Z., Zhang, S., Lim, J.M., Lee, K.O., Li, C., Qian, Q., de Jiang, A., and Qi, Y. (2014). OsMOGS is required for N-glycan formation and auxin-mediated root development in rice (Oryza sativa L.). Plant J. **78:** 632–645.

Wang, X.F., He, F.F., Ma, X.X., Mao, C.Z., Hodgman, C., Lu, C.G., and Wu, P. (2011). OsCAND1 is required for crown root emergence in rice. Mol. Plant **4:** 289–299.

Warthmann, N., Chen, H., Ossowski, S., Weigel, D., and Herve, P. (2008). Highly specific gene silencing by artificial miRNAs in rice. PLoS One **3:** e1829.

Xu, M., Zhu, L., Shou, H., and Wu, P. (2005). A PIN1 family gene, OsPIN1, involved in auxin-dependent adventitious root emergence and tillering in rice. Plant Cell Physiol. **46:** 1674–1681.

Xue, W., Xing, Y., Weng, X., Zhao, Y., Tang, W., Wang, L., Zhou, H., Yu, S., Xu, C., Li, X., and Zhang, Q. (2008). Natural variation in Ghd7 is an important regulator of heading date and yield potential in rice. Nat. Genet. **40:** 761–767.

Yang, L., Jiang, Y., Wu, S.F., Zhou, M.Y., Wu, Y.L., and Chen, G.Q. (2008). CCAAT/enhancer-binding protein alpha antagonizes transcriptional activity of hypoxia-inducible factor 1 alpha with direct protein-protein interaction. Carcinogenesis **29:** 291–298.

Zhang, W., To, J.P., Cheng, C.Y., Schaller, G.E., and Kieber, J.J. (2011). Type-A response regulators are required for proper root apical meristem function through post-transcriptional regulation of PIN auxin efflux carriers. Plant J. **68:** 1–10.

Zhao, Y., Hu, Y., Dai, M., Huang, L., and Zhou, D.X. (2009). The WUSCHEL-related homeobox gene WOX11 is required to activate shoot-borne crown root development in rice. Plant Cell **21:** 736–748.

Zhou, Y., et al. (2009). BC10, a DUF266-containing and Golgi-located type II membrane protein, is required for cell-wall biosynthesis in rice (*Oryza sativa* L.). Plant J. **57:** 446–462.

Zhu, Z.X., Liu, Y., Liu, S.J., Mao, C.Z., Wu, Y.R., and Wu, P. (2012). A gain-of-function mutation in OsIAA11 affects lateral root development in rice. Mol. Plant **5:** 154–161.